Molecular orbital theory.

Roos, Björn; Ryde, Ulf

Published in:
Comprehensive Coordination Chemistry II

DOI:
10.1016/B0-08-043748-6/01245-7

2003

Document Version:
Peer reviewed version (aka post-print)

1 THE MOLECULAR ORBITAL

The molecular orbital (MO) is the basic concept in contemporary quantum chemistry [1, 2, 3]. It is used to describe the electronic structure of molecular systems in almost all models, ranging from simple Hückel theory to the most advanced multiconfigurational treatments. Only in Valence Bond (VB) theory is it not used. Here, polarized atomic orbitals are instead the basic feature. One might ask why the MOs have become the key concept in molecular electronic structure theory. There are several reasons, but the most important is most likely the computational advantages of MO theory compared to the alternative VB approach. The first quantum mechanical calculation on a molecule was the Heitler–London study of H_2 [4] and this was the start of VB theory. It was found, however, that this approach led to complex structures of the wave function when applied to many-electron systems and the mainstream of quantum chemistry was to take another route, based on the success of the central-field model for atoms introduced by by Hartree in 1928 and developed into, what we today know as the Hartree–Fock (HF) method, by Fock, Slater and co-workers (see Ref. [5] for a review of the HF method for atoms). It was found in these calculations of atomic orbitals that a surprisingly accurate description of the electronic structure could be achieved by assuming that the electrons move independently of each other in the mean-field created by the electron cloud. Some correlation was introduced between electrons with parallel spin, through the fulfillment of the Pauli exclusion principle, which required that the total wave function was written as an anti-symmetrized product of atomic spin-orbitals, instead

of a simple product.

At the same time, molecular orbitals were used in simplified treatments of the π-electrons in conjugated organic molecules [6]. Similar empirical or semi-empirical electron structure models were developed and successfully applied in other areas of chemistry. They have been described in other chapters of this book. The field was therefore open for a development of a non-empirical HF theory for molecules. A key paper was published by Roothaan in 1951 [7]. Albeit not first, he gave a clear and detailed description of a HF procedure for molecules that could almost be used as a manual for the development of a computer code. The computers were not quite ready, though, and it was to take another 10 years before the first general-purpose codes were produced.

Today we know that the HF method gives a very precise description of the electronic structure for most closed-shell molecules in their ground electronic state. The molecular structure and physical properties can be computed with only small errors. The electron density is well described. The HF wave function is also used as a reference in treatments of electron correlation, such as perturbation theory (MP2), Configuration Interaction (CI), Coupled Cluster (CC) theory, etc. Many semi-empirical procedures, such as CNDO, INDO, the Pariser–Parr–Pople method for π-electron systems, etc., are based on the HF method. Density Functional Theory (DFT) can be considered as HF theory including a semi-empirical estimate of the correlation error. Hartree–Fock theory is the basic building block in modern quantum chemistry and the basic entity in HF theory is the molecular orbital.

Below we shall describe this model in more detail and study its possibilities

and limitations (because it has serious limitations), but first a few words about electron densities and molecular orbitals in general.

2 THE MANY-ELECTRON WAVE FUNCTION AND THE NATURAL ORBITALS

Building wave functions in molecular quantum chemistry starts from generating a *basis set*, which normally consists of atom-centered functions obtained from calculations on individual atoms. Let us assume that there are m of these atomic orbitals (AOs) and call them $(\chi_p, p = 1, m)$. We can construct the MOs, ϕ_i as a linear expansion in these basis functions (the LCAO method; LCAO = Linear Combination of Atomic Orbitlas). A spin function has to be attached to each molecular orbital and we define the *molecular spin orbitals, (SO)* as:

$$\psi_i = \phi_i \theta_i = \sum_p a_{ip} \chi_p \theta_i \tag{1}$$

The spin function θ_i can take two values (α or β) so with m linearly independent basis functions we can construct $2m$ SOs.

Now, suppose that our system has n electrons. We can then build $N = \binom{2m}{n}$ Slater determinants, Φ_K, by occupying n of the $2m$ SOs in all possible ways. The total wave function, Ψ can be expanded in this *n-electron basis*:

$$\Psi = \sum_K C_K \Phi_K \tag{2}$$

The variation principle can be used to determine the expansion coefficients,

C_K. This leads to the well known secular equation:

$$\sum_L (H_{KL} - \delta_{KL}E)C_L = 0 \tag{3}$$

In the limit of a complete basis set, this equation becomes equivalent to the Schrödinger equation. For a finite basis set, equation (2) represents the best wave function (in the sense of the variation principle) that can be obtained. It is called the *Full CI* (FCI) wave function. It serves as a calibration point for all approximate wave function methods. It is obvious that many of the coefficients in (3) are very small. We can consider most approximate MO models in quantum chemistry as approximations in one way or the other, where one attempts to include the most important of the configurations in (2). We notice that the FCI wave function and energy are invariant to unitary transformations of the MOs. We could actually use the original AO basis set, properly orthonormalized. We may then ask the question whether there is any special representation of the MOs that will concentrate as much information as possible in as few configurations as possible. An answer to this question was given by P.-O. Löwdin in a famous article from 1955 [8], where he gives strong indications that the fastest convergence of the CI expansion is obtained when the orbitals used are the *natural spin-orbitals*.

2.1 The First-Order Density Matrix and the Natural Spin-Orbitals

The probability density of electrons $\rho^{(s)}(x)$ in a quantum mechanical system is given by the diagonal element of the *first-order reduced density matrix*, $\rho^{(s)}(x;x')$ (the superscript s indicates that these quantities depend on the electron-spin:

$$\rho^{(s)}(x;x') = n \int \Psi(x';x_2,x_3...,x_n)^* \Psi(x;x_2,x_3...,x_n) dx_2 dx_3 ... dx_n. \qquad (4)$$

$x_i = (\mathbf{r}_i, \zeta_i)$, where $\mathbf{r}_i$ is the space and ζ_i the spin variable for electron i. If we know this matrix we can compute all one-electron properties of our system. To compute also the two-electron properties, including the total energy, we need to know also the second-order reduced density matrix. We can represent the density matrix in our basis of SOs as:

$$\rho^{(s)}(x;x') = \sum_{i,j} D^{(s)}_{i,j} \psi_i(x')^* \psi_j(x) \qquad (5)$$

The matrix $\mathbf{D^{(s)}}$ is Hermitian and can be brought to diagonal form by a unitary rotation of the orbitals. The new orbitals are called the *Natural Spin-Orbitals (NSOs)*, $\lambda^{(s)}_i$. In terms of them, the density matrix is given as:

$$\rho^{(s)}(x;x') = \sum_{i} \eta^{(s)}_i \lambda^{(s)}_i(x')^* \lambda^{(s)}_i(x) \qquad (6)$$

The quantities $\eta^{(s)}_i$ are called the *occupation numbers* of the NSOs and fulfill the condition: $0 \leq \eta^{(s)}_i \leq 1$ [8].

2.2 Spin Integration and the Natural Orbitals

The electron spin can be separated out in $\rho^{(s)}(x;x')$. If we do that and integrate over the spin variables we obtain the charge density matrix, $\rho(\mathbf{r};\mathbf{r}')$, which we shall also call the 1-matrix. It can be expanded in the MOs:

$$\rho(\mathbf{r};\mathbf{r}') = \sum_{i,j} D_{i,j}\phi_i(\mathbf{r}')^*\phi_j(\mathbf{r}) \tag{7}$$

Again, we can diagonalize the matrix $\mathbf{D}$ and obtain a representation of the 1-matrix in diagonal form:

$$\rho(\mathbf{r};\mathbf{r}') = \sum_{i} \eta_i\lambda_i(\mathbf{r}')^*\lambda_i(\mathbf{r}) \tag{8}$$

The orbitals λ_i are called *Natural Orbitals (NO)*. Their occupation numbers, η_i fulfill the condition: $0 \leq \eta_i \leq 2$.

The natural orbitals have properties that are very stable, independently of how the wave function has been obtained. We find for all molecular systems that the NOs can be divided into three different classes: One group of orbitals have occupation numbers close to 2. These orbitals may be considered as almost doubly occupied. We call them *strongly occupied*. There is another large group of orbitals that have occupation numbers close to zero (typically smaller than 0.02). These are the *weakly occupied* NOs. For stable closed-shell molecules close to their equilibrium geometry, we shall only find these two types of NOs. However, in more complex situations (molecules far from equilibrium geometry, excited states, radicals, ions, etc.) we find a third class of NOs with occupation numbers that are neither small nor close to two. In open-shell systems (radicals, transition-metal compounds, etc.) we find one

or more orbitals with occupation numbers close to one. If we follow a chemical reaction over a barrier we may find cases where an occupation number changes from two to zero while another moves in the opposite direction. An example is given in Fig. 1, which shows how the occupation numbers of the NOs varies when two ethene fragments approach each other and form cyclobutane (the approach is along the symmetry-forbidden reaction path which keeps D_{2h} symmetry).

The figure shows the four orbitals with occupation numbers, which deviate most from two or zero. At large distances they are the π bonding and antibonding orbitals of the two ethene fragments. They have occupation numbers about 1.9 and 0.1, respectively. Close to the transition state for the reaction, one of the bonding orbitals becomes antibonding and weakly occupied, while another orbital becomes bonding and strongly occupied. A picture of the four orbitals in this region is shown in Fig. 2. The two first orbitals have occupation numbers close to one, the third about 1.9 and the fourth 0.1.

At the end of the reaction we have two new bonding orbitals from the ring. They are single bonds, which typically have occupation numbers close to two. The importance of this analysis is that it is valid for the exact wave function. Whether it remains true for approximate methods depends on the method. Below we shall discuss an approach that takes these features of the electronic structure explicitly into account. But first, we shall look closer at the situation where all occupied orbitals have occupation numbers close to two. This situation is common for most molecules in their ground electronic state, close to their equilibrium geometry. It is a natural first approximation

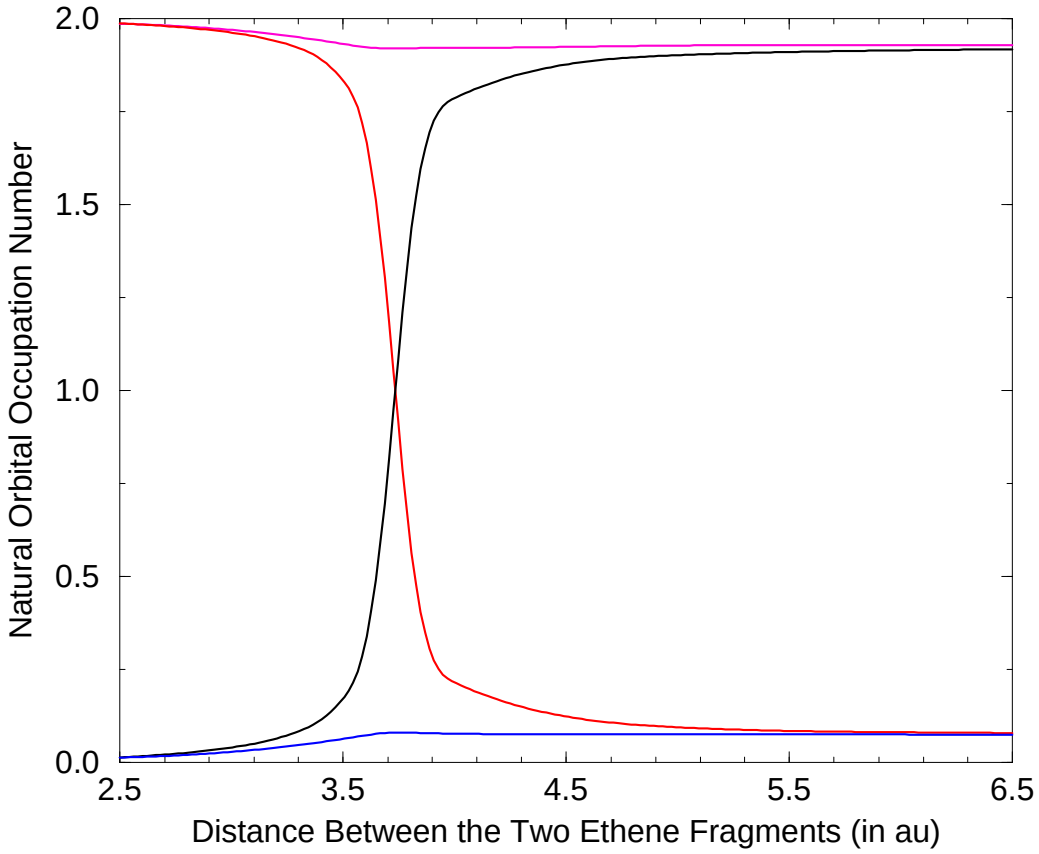

Figure 1: Natural orbital occupation numbers for the active orbitals in C_4H_8 as a function of the distance between the two C_2H_4 fragments. The NOs are shown in Fig. 2. The occupation number profiles of the four orbitals (1-4) have the following colors: black, red, magenta, and blue.

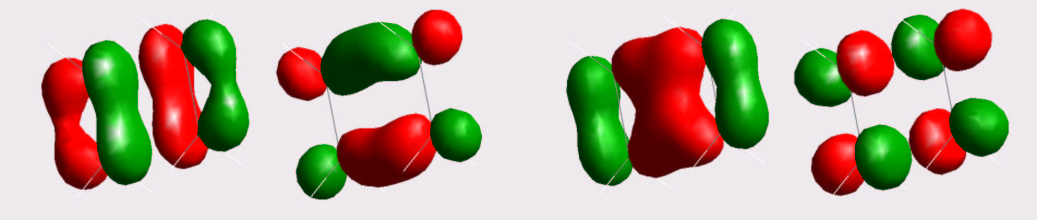

Figure 2: The four natural orbitals in C_4H_8, which change character during the reaction. The distance between the two ethene fragments is 2 Å.

to assume that the occupation numbers are exactly two or zero, which can be shown to be equivalent to assuming that the total wave function is a single configuration (Slater determinant). This is the closed-shell Hartree–Fock model [7].

3 THE HARTREE–FOCK METHOD

The simplest approximation we can make of the full CI expansion of the wave function is to assume that one configuration is enough to describe the wave function. This is equivalent (in the spin-orbital formulation) to select n SOs form the full set. The corresponding wave function is the anti-symmetrized product of these SOs:

$$\Psi_{UHF} = \hat{A}\{\psi_1(x_1)\psi_2(x_2)\cdots\psi_n(x_n)\}, \tag{9}$$

where $\hat{A}$ is the antisymmetrizer ($\hat{A} = \sum_p (-1)^p \hat{P}$; the summation running over all permutations with parity p, $\hat{P}$, of the electron coordinates). In this model, we thus divide the SO space into an occupied and an unoccupied

(virtual) part. Obviously, the quality of this wave function will strongly depend on how we choose the occupied orbitals (in contrast to full CI, which is invariant to this choice). The Hartree–Fock orbitals are those, which makes the energy corresponding to (9) stationary. We shall not attempt to derive the corresponding equations here; the reader is referred to existing literature on the subject (see for example Ref. [9]). The final result is an equation for the orbitals that can be written in the form:

$$\hat{F}\psi_i = \varepsilon_i \psi_i, \tag{10}$$

where $\hat{F}$ is a one-electron operator, which for a molecule has the following form:

$$\hat{F} = \hat{T} + \sum_A \frac{1}{|\mathbf{r} - \mathbf{R}_A|} + \hat{J} - \hat{K}. \tag{11}$$

Here, $\hat{T}$ is the kinetic energy operator and the second term gives the Coulomb attraction between the electron and the nuclei A. The third and fourth terms describe the interaction between one electron and all other electrons. The first of them is the Coulomb operator:

$$\hat{J}\psi_i(x_1) = \int \frac{\rho(x_2; x_2)}{r_{12}} \psi_i(x_1) dx_2 \tag{12}$$

This term is thus completely classical and describes the Coulomb repulsion between an electron in spin-orbital ψ_i and the total electron density ρ. We note that ρ is given in term of the orbitals. The HF equation is thus not linear but has to be solved *self-consistently*, that is, until the input density used to construct $\hat{J}$ equals the output density. The efficiency of current SCF programs lies in their ability to achieve fast convergence in this iterative process and many ingenious convergence procedures have been derived for this purpose.

The second term is the exchange operator. It results from the antisymmetry of the wave function and may be written as:

$$\hat{K}\psi_i(x_1) = \int \frac{\rho(x_2; x_1)}{r_{12}} \psi_i(x_2) dx_2. \tag{13}$$

It is easy to see by inserting the definition (5) of ρ that while all electrons contribute to $\hat{J}$, only those with the same spin as ψ_i will be included in $\hat{K}$. It may be shown that this contribution to the total energy is negative. The exchange terms thus lowers the energy of the system, because electrons with parallel spins avoid each other, resulting in a reduction of the repulsion. The antisymmetry of the wave functions results in zero probability for finding two electrons with the same spin in the same point in space. This is the so called Fermi hole. The HF model does not prevent electrons with opposite spins to occupy the same point in space, which has important consequences for the energy error of the HF model, the so called *correlation energy*. It arises mainly from the interaction of pairs of electrons with opposite spins and can to a good approximation be written as a sum of pair energies. The success of second-order perturbation theory (MP2) for computing the correlation energy is based on this property of the HF wave function.

We also notice that the exchange operator is non-local, because the results depend on the value of ψ_i in all points in space. One of the challenges in DFT theory is to model the non-local exchange with a local operator.

The eigenvalue of the HF orbital ψ_i, ε_i, can be identified as an energy of the electron in that orbital. The background is Koopmanns' theorem that states

that removing one electron from an occupied orbital, without modifying the remaining ones, results in an energy increase $-\varepsilon_i$, thus relating the eigenvalues of the occupied orbitals to the ionization energies of the molecule. In the same way it may be shown that the energies of the virtual orbitals give a measure of the electron affinity. It is important to emphasize that these relations are only approximate because they do not include relaxation of the density and electron correlation effects. They are nevertheless important conceptually because they give a model of the electronic structure where the electrons move in well-defined molecular orbitals with an equally well defined orbital energy. This is the shell model for molecules, except for one little detail.

The formalism given above assigns one spin orbital to each electron. In principle they all have different space parts. However if you perform such a calculation for the water molecule, you will find that orbitals for α and β spin are pairwise identical. The result is 5 occupied MOs, each with two electrons of opposite spin. The concept of the closed shell is thus a result in HF theory. Not all molecules behave in this way, but many do so when they are close to their equilibrium geometry. The pairing is self-consistent for an even number of electrons, that is, if the electrons are paired in identical orbitals, the HF equation for α and β spin orbitals will be identical and thus give a paired solution. The only question is whether the solution is stable (is a minimum). It may be shown that this property of the solution is related to the energy difference between the closed-shell state and the lowest triplet state. When this energy is too low, the paired solution becomes unstable and another solution with different orbitals for different spins appears with a lower energy. Such a wave function is no longer an eigenfunction of the total

spin and may also break the molecular point-group symmetry.

A closed-shell structure for a ground-state molecular wave function is only possible for an even number of electrons. An open shell will always lead to spin-polarization, that is, different orbitals for different spins for all electrons. The model with this property is called *Unrestricted Hartree–Fock, UHF*. It is possible to impose the restriction of pairing also for open-shell systems, but this is then an additional condition that will lead to a higher energy than the corresponding UHF solution. Such an approach is called *Restricted Hartree–Fock, RHF*. It may be constructed in such a way that the wave function is an eigenfunction of the total spin, which is not a property of the UHF approach [10]. However, as we shall discuss below, open-shell systems need in general a higher order treatment, where more than one determinant is used to expand the wave function.

The HF approach is surprisingly accurate for normal closed-shell molecules involving only light (first and second-row) atoms. Bond distances are usually represented with an accuracy of 0.02 Å or better and the accuracy in bond angles is a few degrees. Physical properties like dipole moments, etc. are predicted with errors of the order of 10%. For an extensive error analysis of different quantum chemical methods see for example Ref. [11]. It should be noticed, however, that for systems including heavier atoms, the errors may be larger also when the system is a closed-shell. A typical example is ferrocene, where the metal–ring distance is overestimated with 0.23 Å at the HF level [12]. The error can be related to strong electron correlation effects in the $3d$ shell of iron. Thus, one cannot use the HF approach with confidence for

studies of coordination compounds. Electron correlation has to be invoked already when the wave function is determined.

HF theory cannot be used to compute properties the are related to processes where electron pairs are formed or broken. The correlation error depends strongly on the number of such pairs. Examples of such processes are dissociation of a chemical bond, ionization, excitation, passing a transition state in a chemical reaction, etc. The possible applications of HF theory are thus severely limited. Methods to compute the correlation energy starting from a HF reference wave function are described in several articles in this book. The most commonly used methods today for ground-state systems are probably second-order perturbation theory and density functional theory.

However, in several cases it is not possible to use HF theory at all. It is based on the assumption that the natural orbitals have occupation numbers close to either two of zero (in the closed-shell case). We saw in the example of C_4H_8 that this is not always the case. Some orbitals may drastically change their occupation during a chemical process. In strongly correlated systems, like some transition metals, the HF method might give large errors even if the occupation numbers are not very different from zero, one or two. In such cases it is necessary to extend the theory and allow for occupation numbers different from two or zero.

4 ACTIVE ORBITALS AND MULTICONFIGURATIONAL WAVE FUNCTIONS

Let us take a closer look at the $C_2H_4 + C_2H_4 \rightarrow C_4H_8$ reaction. Why do the orbitals change their occupation numbers? Let us introduce the following notations:

- ϕ_1 ethene bonding but antibonding between the two (orbital 1 in Fig 2)
- ϕ_2 ethene antibonding but bonding between the two (orbital 2)
- ϕ_3; bonding between all four carbons (orbital 3)
- ϕ_4; antibonding between all four carbons (orbital 4)

At large distances between the two moieties, the orbitals ϕ_1 and ϕ_3 will be doubly occupied. This gives a wave function that we symbolically can write as (forgetting all other electrons):

$$\Psi_1 = (\phi_1)^2(\phi_3)^2 \tag{14}$$

When cyclobutane has been formed the two orbitals that form the new bonds, ϕ_2 and ϕ_3, will instead be occupied and we get the wave function:

$$\Psi_2 = (\phi_2)^2(\phi_3)^2 \tag{15}$$

So, orbital ϕ_3 is always occupied and its occupation number changes only little during the reaction. Orbital ϕ_4 is always weakly occupied. Orbitals ϕ_1 and ϕ_2, however, change their occupation, ϕ_1 from zero to two and ϕ_2 in the opposite way.

What will happen to the energies along the reaction path for these two HF configurations. The energy surface for Ψ_1 will clearly become repulsive when

the two ethene molecules approach each other, because ϕ_1 is antibonding. Ψ_2 will on the other hand become repulsive when we dissociate the new bonds, since this configuration cannot give the ethene double bonds. The electronic configuration will have to change from Ψ_1 to Ψ_2 at some point along the reaction path. This will happen at the point where the two potentials cross, that is, where they have the same energy. If they are used as basis functions in a two-by-two CI calculation one obtains:

$$\Psi = \frac{1}{\sqrt{2}}(\Psi_1 - \Psi_2) \tag{16}$$

The natural orbitals of this wave function will be the same, but now ϕ_1 and ϕ_2 will have the occupation number one. This is the crossing point shown in Fig. 1. So, we have three wave functions: (14), valid at infinite distance, (15) valid at the C_4H_8 equilibrium geometr and (16) valid in the transition state region. How do we write a wave function that is valid for the full reaction path. The obvious choice is to abandon the single-configuration (HF) approach and write:

$$\Psi = C_1\Psi_1 + C_2\Psi_2 \tag{17}$$

and determine not only the orbital but also the configuration mixing coefficients by the variation principle. The example illustrates a chemical process where we need to go beyond the single-determinant approach in order to understand the electronic structure. But note that the basic quantity is still the natural orbitals. It is obvious that this example illustrates a whole class of chemical processes: chemical reactions that involve a change of electronic configuration.

Let us take another example, which is of interest in coordination chemistry. It concerns the nickel atom and its lower excited states. The ground state is ^3D $(3d^9 4s)$, but 0.03 eV higher is ^3F $(3d^8 4s^2)$. These values are averaged over the J components. 1.70 eV higher we find the closed shell ^1S $(3d^{10})$ state. If we compute these relative energies at the RHF level, we find $\Delta E(^3D \rightarrow ^3F) = -1.63$ eV and $\Delta E(^3D \rightarrow ^1S) = 4.33$ eV. It turns out to be very difficult to compute these energies accurately (see for example [13] for a discussion of results at different levels of theory). The reason is strong radial correlation effects in the (almost) filled $3d$ shell. Actually, it was early noted for the copper atom that a large fraction of the correlation energy could be recovered if an electron configuration $4s3d^9 3d'$ was used instead of $4s3d^{10}$ [14]. This *double-shell* effect has been found to be important for a quantitative understanding of the electronic spectra of transition metals with more than a half filled d-shell, not only for free atoms but also for complexes [15]. The occupation numbers of the orbitals in the second d-shell are not very large (of the order of 0.01–0.02) but their contribution to the energy is large. The example shows that there is not always a trivial relation between the occupation numbers and the importance of a natural orbital for the description of the electronic structure and the energetics of a molecular system.

How can we extend Hartree–Fock theory to incorporate the effects of the most important natural orbitals even in cases where the occupation numbers are not close to two or zero. Actually, Löwdin gave an answer to this question in his 1955 article, where he derived something he called the *extended Hartree–Fock equations* [8]. The idea was to use the full CI wave function (2), but with a reduced number of orbitals, and determine the expansion coefficients

and the molecular orbitals variationally. His derivation was formal only and had no impact on the general development at the time. It was only 20 years later that a similar idea was suggested and developed into a practical computational procedure. The approach is today known as the *Complete Active Space SCF method, CASSCF* [16].

The CASSCF method is based on some knowledge of the electronic structure and its transformation during a molecular process (chemical reaction, electronic excitation, etc.). This knowledge can, if necessary, be achieved by making experiments on the computer. Let us use C_4H_8 as an example. We noticed that four of the MOs in this molecule will change their occupation numbers considerably along the reaction path. Four electrons are involved in the process. We shall call these orbitals *active*. The other electrons remain in doubly occupied orbitals. Such orbitals will be called *inactive*. The inactive and active orbitals together constitute a subset of the MO space. Remaining orbitals are empty. We can define configurations in this subspace by occupying the four active orbitals with the four electrons in all possible ways. It is left to the reader to show that the number of such configurations with the spin quantum number zero (singlet states) is 20. The number of Slater determinants is $\binom{8}{4} = 70$, which includes, in addition to the singlet states, 3×15 triplet and 5×1 quintet states. Of the 20 singlet configurations, only 8 have the correct symmetry. The wave function is thus in this case a linear combination of these 8 configuration functions (CFs). Above, we discussed the electronic structure in terms of only two CFs, so it is clear that we do not need to invoke all eight functions. However, the selection of individual configurations to use in the construction of the total wave function

is a complicated procedure that easily becomes biased. The CAS approach avoids this by only specifying the inactive and active orbitals.

The choice of the active orbitals is in itself non-trivial. Again, we can use C_4H_8 as an example: we chose the four orbitals that changed character along the reaction path. Two of them are C–C σ-bonding in the final molecule and the other two are antibonding in the same bonds. Thus we have a description where two of the bonds are described by two orbitals each, while the two other C–C bonds (those of the original ethene moieties) are inactive. If we optimize the geometry of the C_4H_8 molecule with such an active space we shall find it to be rectangular and not quadratic. The D_{4h} symmetry of the molecule demands that the four C–C bonds are treated in an equivalent way. Thus we need an active space consisting of eight orbitals and eight electrons. The resulting wave function will comprise 1764 CFs, which will be reduced to a few hundred due to the high symmetry.

4.1 Bond Dissociation

Another example that illustrates the breakdown of the HF approximation, concerns the dissociation of a chemical bond. Assume that two atoms A and B are connected with a single bond involving two electrons, one from each atom. To a good approximation we can describe the bond with the electronic configuration $\Psi_1 = (\sigma)^2$, where

$$\sigma = N(\sigma_A + \sigma_B) \tag{18}$$

and σ_A and σ_B are two atomic orbitals, one on each atom. This wave function is, however not valid at large interatomic distances, because it contains ionic terms, where both electrons reside on the same atom. Here, the wave function is better described in terms of the localized orbitals:

$$\Psi_\infty = (\sigma_A(1)\sigma_B(2) + \sigma_A(2)\sigma_B(1))\Theta \tag{19}$$

Where Θ is a spin function for a singlet state with two electrons. This wave function can also be written as:

$$\Psi_\infty = \frac{1}{\sqrt{2}}(\Psi_1 - \Psi_2) \tag{20}$$

where Ψ_1 is the bonding configuration given above and $\Psi_2 = (\sigma^*)^2$, where σ^* is the *antibonding* orbital:

$$\sigma^* = N^*(\sigma_A - \sigma_B) \tag{21}$$

Thus, the wave function is described by two electronic closed-shell configurations at infinite distance between the atoms. The situation is actually identical to what was obtained in the transition-state region for the cyclobutane reaction. The reason is also the same: The two configurations $(\sigma)^2$ and $(\sigma^*)^2$ become degenerate at dissociation and will mix with equal weights. It is clear that a wave function that describes the full potential curve for the dissociation of a single bond should have the form:

$$\Psi = C_1\Psi_1 + C_2\Psi_2 \tag{22}$$

The two natural orbitals σ and σ^* will have the occupation numbers $\eta = 2C_1^2$ and $\eta^* = 2C_2^2$, respectively. At infinite distance they will both be one but

near equilbrium almost all of the occupation will reside in the bonding orbital. For weak bonds, an intermediate situation obtains and we can actually define a bond order, BO, from the natural orbital occpuation numbers:

$$BO = \frac{\eta - \eta^*}{\eta + \eta^*} \tag{23}$$

which becomes one when η^* is zero and zero when both are one.

An illustration of a more complicated multibonding situation is given by the chromium dimer. Here, six weak bonds are formed between the $3d$ and $4s$ orbitals of the two Cr atoms. CASSCF calculations with 12 electrons in the 12 valence orbitals gives the following NO occupation numbers at the equlibirium geometry:

Orbital pair	Bonding	Antibonding	Bond order
$4s$	1.890	0.112	0.89
$3d\sigma$	1.768	0.227	0.77
$3d\pi$	3.606	0.394	1.61
$3d\delta$	3.134	0.868	1.13

The computed total bond order, using the formula given above, is 4.4. Effectively, two Cr atoms form a quadruple bond even if all twelve electrons are involved. One notices that the occupation number of the antibonding $\delta-$orbital is large, indicating a weak bond only. In Fig. 3 we show how the NO occupation numbers vary with the interatomic distance.

The vertical line indicates the equilibrium distance. We can see how the $4s$ bond is formed at larger distances than the $3d$ bonds and also that the 3dσ and 3dπ bonds are stronger than the 3dδ bond [17].

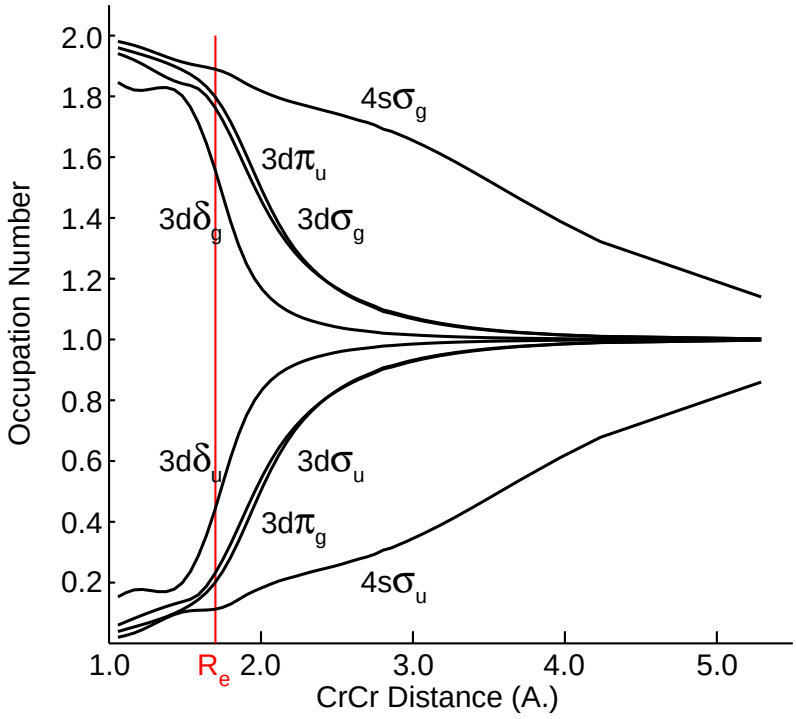

Figure 3: Natural orbital occupation numbers for the bonding and antibonding orbitals in Cr_2 as a function of the distance between the two atoms.

The general conclusion we can draw from the above exercises is that in order to describe the formation of a chemical bond, we need to invoke both the bonding and antibonding orbitals. It is only for strong bonds close to equilibrium that the bonding orbital dominates the wave function.

Another conclusion we can draw is that if we are in a situation where two or more electronic configurations (of the same symmetry) have the same or almost the same energy, they will mix strongly and a quantum mechanical model that only takes one of them into account will not be valid.

4.2 The Complete Active Space SCF Model–CASSCF

The CASSCF model has been developed to make it possible to study situations with near-degeneracy between different electronic configurations and considerable configurational mixing. In Fig. 4 we illustrate the partitioning of the orbital space into inactive, active and virtual.

The wave function is a full CI in the active orbital space. By using spin-projected configurations we can select those terms in the full CI wave function that have a given value of the total spin. When the system has symmetry, we can also add the condition that the selected terms shall belong to a given irreducible representation of the molecular point group. The wave function will then be well defined with respect to these properties. It will considerably reduce the length of the CI expansion. In the example of C_4H_8 we could decrease the size from a total of 70 CFs to 8 by selecting only the terms for which $S = 0$ (singlets) and which belong to the totally symmetric

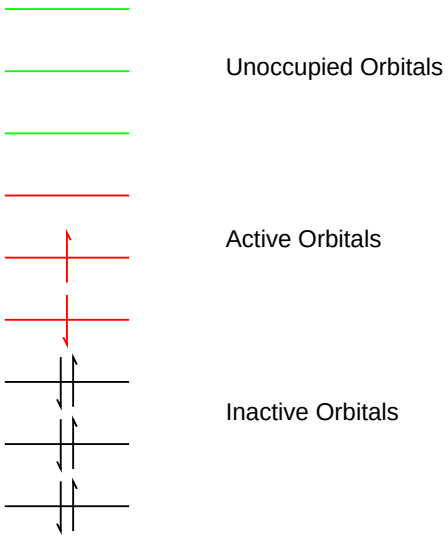

Figure 4: The partitioning of the orbital space into inactive, active and virtual in the CASSCF method.

representation of the D_{2h} point group. Apart from these restriction, our wave function is completely general. It may contain an arbitrary number of open shells and it may belong to any of the irreducible representations of the point group. With the CASSCF approach it becomes equally simple to study the potential of the $^{13}\Sigma_g^+$ state of Cr_2 as it is to study the $^1\Sigma_g^+$ ground state (both dissociate to ground state Cr atoms).

We shall not discuss here in any detail how one proceeds to optimize a CASSCF wave function. The reader is referred to the existing literature [11, 16, 18]. Instead we shall continue with some study cases to illustrate how the multiconfigurational approach is used in practical applications. But, before that, a few words about the remaining error.

The CASSCF model allows us to include into the wave functions contributions from the most important NOs that describe the most important correlation effects among the electrons. This type of correlation if often called *static* or *non-dynamic*. It is usually long range and describes effects on the electronic structure leading to separation of the electrons in a pair. Typical examples are dissociation of a chemical bond or the C_4H_8 reaction described above. This partitioning of the electron correlation is not strict, as is illustrated by the Ni atom, where the separation of the electrons through the introduction of a second $3d-$shell is not long range. The remaining error is called *dynamic correlation* and is caused by the instantaneous correlation of electrons in the region where the inter-electronic distance is close to zero – the cusp region. It can be treated by the CASSCF method only for very small molecules with few electrons because a large number of NOs is needed

for an accurate description. A thorough discussion of the convergence of the dynamic correlation energy in CI like methods may be found in Ref. [11].

Only a few accurate methods exist today for the treatment of the dynamic correlation energy in cases where the non-dynamic effects are large. For systems where Hartree–Fock theory is adequate, a number of different approaches exist, the most accurate being coupled-cluster (CC) theory. The most commonly used approach for large molecules is probably Møller–Plesset second-order perturbation theory, MP2. We again refer to Ref. [11] for a detailed discussion of these methods. They are all based on a HF reference function. DFT may also be considered to belong to this type of methods, even if it is not so clear how well this method will work in the case of near-degeneracy. Some applications indicates that it might work reasonably well, but others give less accurate results.

It has not yet been possible to extend the CC approaches in a systematic way to the multi-configurational regime. For small molecules it is in this case possible to use large multi-reference CI methods, where the most important configurations in a CASSCF wave function is used as reference functions and the CI expansion comprise all single and double excitations form the occupied orbitals to virtual or other (partially) occupied orbitals. The size to such a CI expansion grows, however, too quickly to be of interest for larger molecules.

An alternative approach was developed about ten years ago. It may be regarded as an extension of the MP2 method to the case where the reference function (the zeroth-order approximation) is not a HF but a CASSCF wave

function [19, 20, 21]. It has been named CASPT2. We shall not describe the method in detail here, but it will be used in the illustrations discussed below. The accuracy is limited by the possibility to choose an adequate active space for the CASSCF wave function and by the fact that the remaining correlation effects are only treated to second order in perturbation theory. Nevertheless, it has been used successfully in a large number of studies of a variety of properties of ground and excited states in organic and inorganic molecules and coordination compounds involving transition metals, lanthanides and actinides. Also metal containing active sites in proteins have been studied. We shall below give a few examples.

5 THE COORDINATION OF NICKEL WITH ETHENE

As a first example we use the complex formed between a nickel atom and the ethene molecule. This compound is a prototype for coordination of a transition metal to a double bond in an organic molecule. It is traditionally understood in terms if the Dewar–Chatt–Duncanson (DCD) model [22, 23] where the bonding is described as donation of electrons from the ethene $\pi-$orbital to Ni and a corresponding back-donation from Ni($3d$) to the π^*-orbital. However, it is not obvious that the binding may be described in such a simple model, because there is no empty Ni orbital into which electrons may be donated. The dissociation of the molecule gives Ni in the $3d^9 4s$, ^1D, state with one occupied $4s$ orbital, which would prevent an effective back-

donation. A number of studies of this compounds have been performed using the CASSCF/CASPT2 method [24, 25, 26]. From these studies a somewhat more complex picture of the bonding has emerged, which is not in conflict with the DCD model, but explains how the problem with the 4s orbital is solved by the bonding mechanism. This explanation is multiconfiguration in nature and resembles in a way our preceding discussions about how a configuration changes to another one in the course of a chemical reaction. Let us take a closer look at these results. The molecule has C_{2v} symmetry with nickel bonded at the center of the C–C bond perpendicular to the ethene plane.

The Ni atom in its ground state has one singly occupied $3d$ and one $4s$ orbital coupled to a singlet. The situation resembles two radicals, but here we have both electrons on the same atom. With two radicals we can form the bonding and antibonding combination of the localized radical orbitals and write the wave function as a linear combination of two configuration as was discussed above in the section on bond dissociation (equation (16)). We can do the same here and form the orbitals $3d+4s$ and $3d-4s$. The wave function then has the symbolic form:

$$\Psi = C_1(3d+4s)^2 + C_2(3d-4s)^2, \tag{24}$$

with $C_1 = -C_2 = \frac{1}{\sqrt{2}}$. This is an equally valid representation of the ^1D state. The $3d+4s$ orbital is the hybrid that points towards the C–C bond of the ethene molecule, while the other hybrid points away from ethene.

The coefficient C_1 will start to decrease when the nickel atom approaches the ethene double bond, while C_2 will increase to a value close to one. Thus,

the electron pair, which causes the repulsion is moved out of the way and binding can take place between the $3d+4s$ orbital on Ni and the $\pi-$orbital on ethene. The two orbitals are shown in Fig. 5 as $9a_1$ and $10a_1$ (bottom left). It is evident from the shape of $9a_1$ that a rather covalent bond is formed. The occupation number of this orbital is close to two, because there is no low-lying orbital that can be used for correlation.

The second bond is formed between the $3d_{xz}$ orbital (xz is the NiCC plane) and the empty ethene π^*-orbital. This bond is also quite covalent (orbital $5b_2$ in the figure) but weaker. The occupation number is 1.91 with 0.09 electrons in the corresponding antibonding $6b_2$ orbital. The other orbitals in Fig. 5 are the doubly occupied $3d$ orbitals of Ni and the corresponding correlating orbitals, the $3d'$ orbitals of the Ni double shell. It can be seen from the pictures that the latter orbitals occur in pairs with the $3d$ orbitals and have a clear $4d$ character.

The covalency of the Ni–ethene bond is a result of the multiconfigurational treatment. The charge of the Ni atom at the HF level is +0.9, which reduces to +0.5 when the extra NOs are added. For a more detailed discussion of the bonding, including also a discussion of the bond energy, we refer to the original article [26]. What we have seen here is another example of the need of a multiconfigurational treatment for the complete understanding of the binding mechanism.

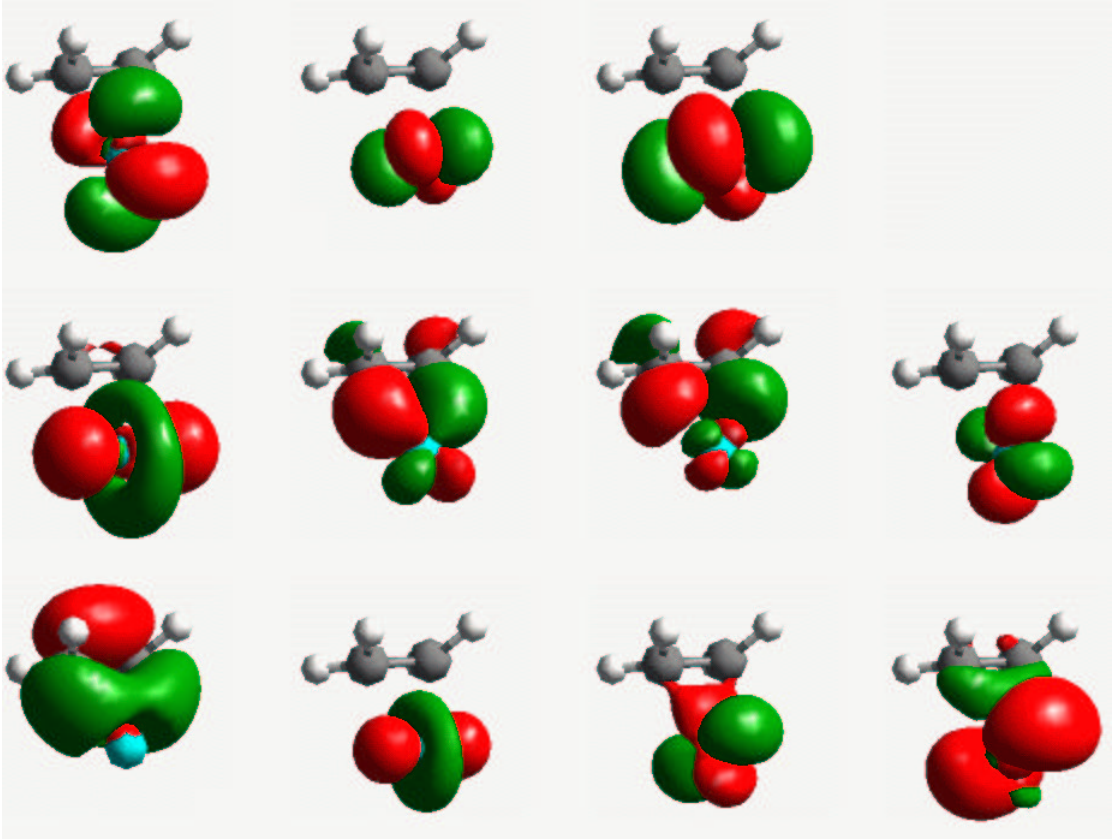

Figure 5: Natural orbitals in the NiC_2H_4 molecule. Counted from left to right and from bottom up, the orbitals are (occupation numbers within parenthesis): $9a_1$ (2.00), $10a_1$ (1.98), $11a_1$ (1.97), $12a_1$ (0.03), $13a_1$ (0.02), $5b_2$ (1.91), $6b_2$ (0.09), $4b_1$ (1.98), $5b_1$ (0.02), $2a_2$ (1.98), $3a_2$ (0.02).

6 THE FERROCENE MOLECULE

As a second example of the coordination of a transition metal to carbon, we shall look at the binding in another prototype molecule, ferrocene. This molecule was a challenge to ab initio quantum chemistry for a long time because of the difficulty to compute the iron–ring distance. Calculations at the HF level overestimate this distance with as much as 0.20 Å. Adding correlation at the MP2 level leads instead to a distance that is 0.17 Å too short [26]. Only highly correlated calculations, which includes all valence electrons, the semi-core of Fe, and the dispersion interaction between the two cyclopentadienyl rings, was able to reproduce the experimental bond distance [26, 27]. Here we shall not discuss these problems in detail, but only illustrate how the bonding mechanism is described in a multiconfigurational approach. It should be mentioned, however, that when the most important NOs are included in the wave function (as described below) the bond distance is reduced from 1.86 Å (SCF result) to 1.72, now only 0.06 Å longer than the experimental value. Thus, a semi-quantitative result may be obtained already at this level of theory. Higher accuracy can only be obtained by adding dynamical correlation effects. Before starting the discussion of the electronic structure it might be of some interest for the reader to show in some detail how the calculations of the NOs were performed. We therefore give below computational details.

6.1 Computational Details

A new set of calculations were performed for the present discussion. They were done on a Linux equipped laptop. The MOLCAS quantum chemistry software was used [28]. The basis set was of the Atomic Natural Orbital type (ANO-L of the MOLCAS library [29, 30]). The ANOs are well suited for multiconfigurational calculations, because they have been determined from correlated calculations on the atoms. Thus, the basis set contains functions that are optimized for atomic correlation. For iron, the basis set contained 7 s-type, 6 p-type, 3 d-type and 1 f-type ANOs. $3s2p1d$ was used for carbon and $2s1p$ for hydrogen. This is a rather limited basis set. It cannot be used to compute energy-related quantities, but for the present purpose of demonstrating the NOs and their occupation, it is satisfactory. The geometry chosen was from an earlier study [26]: Fe–ring distance = 1.643, r(C–C)=1.423, and r(C-H)=1.086 Å. The symmetry of the molecule is D_{5h}. In practice C_{2v} was used, but the full symmetry was preserved in the calculation.

A CASSCF calculation was performed with input orbitals from a preceding SCF calculation. The active space was chosen according to the 10-electron rule: The five $3d$ orbitals were first chosen. For each doubly occupied orbital, an empty correlating orbital of the same symmetry was added. This can either be a $3d'$ orbital (the double shell), an empty ligand orbital (π^* from the ring), or a combination of both determined by the CASSCF orbital optimization procedure. For each empty $3d'$ orbital an occupied ligand orbital of the same symmetry was added. This gives and active space with 10 electrons in 10 orbitals. This way of selecting active orbitals for a coordination compound

is quite general. It was used above for NiC_2H_4. More examples and a more detailed discussion may be found in Ref. [15].

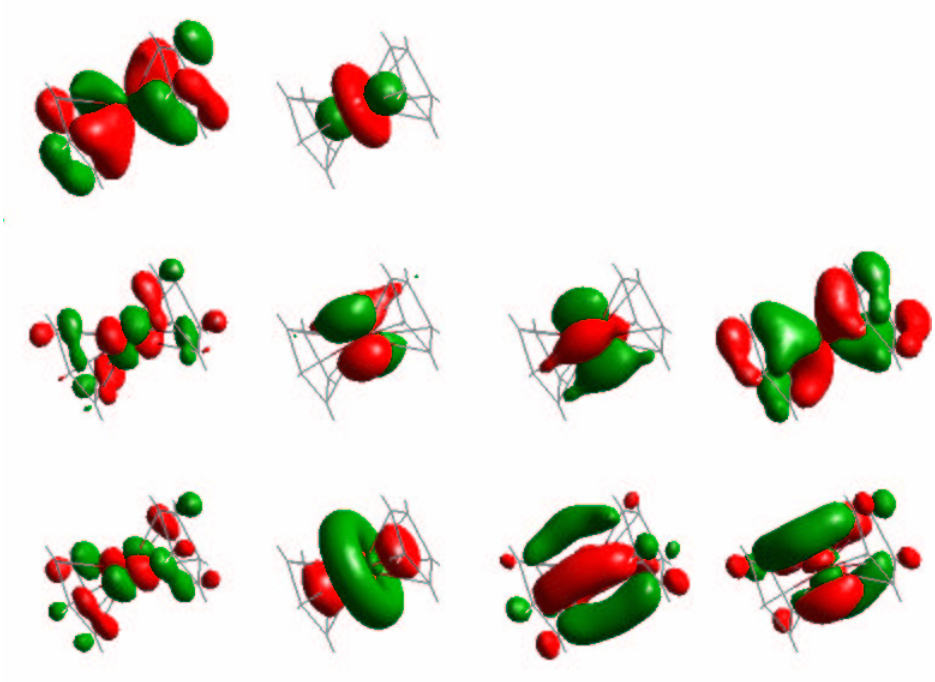

Figure 6: Natural orbitals in the Ferrocene molecule. Counted from right to left and from top down, the orbitals are (occupation numbers within parenthesis): $8a_1'(1.96)$, $4e_1''(1.95)$, $4e_1''(1.95)$, $4e_2'(1.94)$, $4e_2'(1.94)$, $5e_1''(0.07)$, $5e_2'(0.05)$, $5e_2'(0.05)$, $9a_1'(0.03)$, $5e_1''(0.07)$.

6.2 The Electronic Structure of Ferrocene

Fe^{2+} has the electronic configuration $(3d\sigma)^2(3d\delta)^4$ in ferrocene, where we have assumed that the z-axis is the five-fold symmetry axis. Rewritten in the D_{5h}

symmetry it is $(a_1')^2(e_2')^4$. The empty $3d$ orbitals are $3d\pi$ (e_1''). The 10 ligand $\pi-$orbitals have the symmetries: a_1', a_2'', e_1', e_1'', e_2' and e_2'' with the following occupation: $(a_1')^2(a_2'')^2(e_1')^2(e_1'')^2$. Following the recipe give above we thus choose the following active space (introducing also the correct numbering of the orbitals). $(8,9)a_1'$, $(4,5)e_1''$ and $(4,5)e_2'$.

What bonding mechanism will this active space result in. Let us first look at the doubly occupied $3d-$orbitals. $8a_1'$ will only interact repulsively with the ring because the ring $\pi-$orbital of the same symmetry is also occupied. We thus expect a rather isolated orbital and the correlating orbital $9a_1'$ will then describe the double shell effect and also be localized to iron. The orbitals are shown in Fig. 6. They have the expected shape.

The situation is different for the four electrons in the $4e_2'$ orbital pair. The correlating orbital is now the empty ligand orbital pair $5e_2'$. Back-transfer from Fe to the rings is thus possible and a bonding and antibonding pair or orbitals may be formed. As can be seen from the picture, the delocalization is rather limited in the doubly occupied orbital. The corresponding correlating orbital pair $5e_2'$ is partly $4d$ in character but shows also an interesting ring–ring bonding feature, which would be absent in a staggered conformation. The total population in this pair is 0.11 electrons.

The $4e_1''$ orbital pair should be mainly located on the rings. It is, however, extensively delocalized onto the $3d\pi$ orbitals and an almost covalent bond is formed. The Mulliken population analysis gives 0.74 electrons in each of the $3d\pi$ orbitals. The corresponding correlating pair is a mixture of $4d$ and ring $\pi-$orbitals. It has a total occupation of 0.14 electrons.

In total, 0.27 electrons are moved from the strongly to the weakly occupied orbitals, thus illustrating the difference in the picture of the bonding that the CASSCF model gives compared to HF. It is interesting to see that quite a redistribution occurs among the $3d-$electrons. The Mulliken population analysis gives a total of 6.78 electrons in these orbitals to be compared to 6 in the free ion (note that the populations also include the correlating $4d$ orbitals). Of these, 1.48 goes into the $3d\pi-$orbitals, which are empty in the free ion and 0.53 electrons are moved out of the $3d\delta-$orbitals. The total charge of the Fe atom is +0.82. The difference between this number and the total number of $3d-$electrons is due to the population of $4p$.

The multiconfigurational picture of the electronic structure in ferrocene shows a molecule with (of course) strong ionic bonding, but in addition prominent covalent features, mainly arising from ligand to metal charge transfer from the filled ligand orbitals of e_1'' symmetry to the corresponding empty $3d\pi-$orbitals. The bond is reasonably strong with an antibonding population of 0.07 in each orbital of the degenerate pair. One pair of weakly occupied orbitals also exhibits pronounced ring–ring bonding. There is a clear difference between this picture and the one obtained at the SCF level, which gives an ion more similar to free Fe^{2+}. The number of electrons in the different $3d-$orbitals is at that level of theory: 1.89 ($3d\sigma$), 0.94 ($3d\pi$), and 3.78 ($3d\delta$). The most pronounced difference is found in the population of the bonding $3d\pi-$orbitals.

7 THE $[Re_2Cl_8]^{2-}$ ION

This ion was one of the prototypes of multiple bonding between two transition metal ions. It was discovered and characterized in 1965 by Cotton and Harris [31]. The Re–Re bond distance was determined to be only 2.24 Å and it was concluded that it is a quadruple bond. A similar short bond had earlier been found in the tri-nuclear complex $[Re_3Cl_{12}]^{3-}$ [32]. These ions were to form the conceptual basis for the forthcoming development of the field multiple metal–metal bonding in transition metal chemistry.

So, is there really a quadruple bond between the Re atoms in $[Re_2Cl_8]^{2-}$. In 1965 it was impossible to give a final theoretical answer to this question. The theoretical models that could be used were not advanced enough. The multiconfigurational approach we have access to today is, however, capable of giving a conclusive answer to the question. We know from the preceding discussion that a single bond is formed when the occupation number of the bonding orbital is close to two, while the corresponding antibonding orbital has a small occupation number. The ion has been studied in recent extensive CASSCF/CASPT2 calculations, which involve an optimization of the ground-state geometry, a characterization of the electronic structure and a detailed analysis of the electronic spectrum [33]. The calculation used a large relativistic ANO basis set and included spin-orbit coupling. We refer to the full article for all details. Here we shall only present the NOs and see what they tell us about the nature of the chemical bond.

Rhenium appears in the complex as Re^{3+} with the electronic configuration

$(5d)^4$. If we place the z-axis along the Re–Re bond and the Cl ions in the planes bisecting the xz- and yz-planes, we can write the configuration as $(5d_{z^2})(5d_{x^2-y^2})(5d_{xz})(5d_{yz})$ with all spins parallel. The $(5d_{xy})$ orbital is empty because of the interaction with the Cl $3p$ orbitals. We can thus, in principle, form a quadruple bond between the two Re ions. Cotton noted already in 1965 that this bonding pattern explains the eclipsed structure of the ion, which allows one of the the $3d\delta$ orbitals to be involved in the Re–Re bonding [34].

Let us now perform a CASSCF calculation with all the $5d$ orbitals active and in addition the two Cl orbitals that interact with $(5d_{xy})$. This gives 12 orbitals and 12 electrons. We perform the calculation in D_{2h} symmetry but can classify the orbitals using the full D_{4h} point group.

The resulting NOs are shown in Fig. 7 with their occupation numbers (the active orbitals are for simplicity numbered from one up). We can clearly see the pairing of orbitals into bonding and antibonding. The sum of the occupation numbers for each such pair is very close to 2.0. Most strongly occupied are the two Re-Cl bonding orbitals, which, involve the $5d_{xz}$ metal orbital. The two orbitals are mainly located on the Cl ions but a population analysis gives a gross atomic population of 0.7 for each of the $5d_{xz}$ orbitals. The occupation numbers are close to two. The two corresponding antibonding orbitals (bottom right in the figure) are mainly $5d_{xz}$ in character and are only weakly populated.

The remaining eight orbitals in the figure describe the Re–Re bond. Most strongly bonding is, as expected, the $\sigma-$orbital, $1a_{1g}$, which has an occupa-

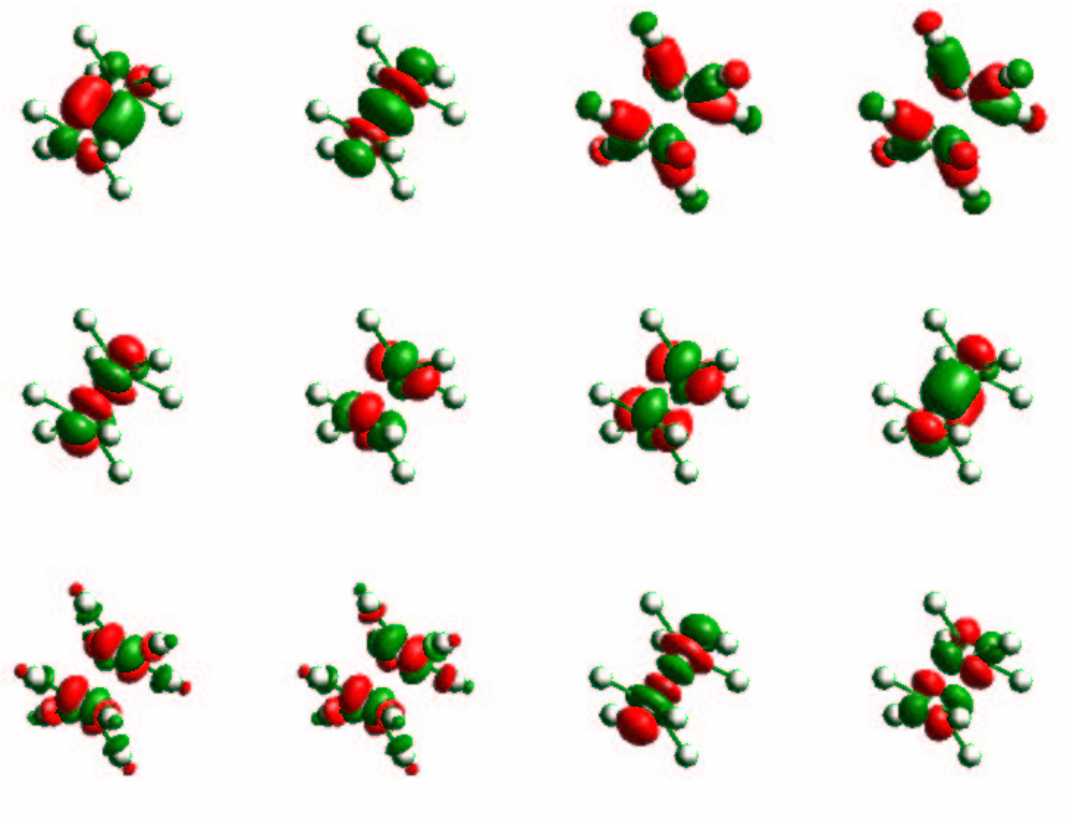

Figure 7: Natural orbitals in the $[Re_2Cl_8]^{2-}$ ion. Counted from right to left and from top down, the orbitals are (occupation numbers within parenthesis): $1b_{1u}(1.98)$, $1b_{1g}(1.98)$, $1a_{1g}(1.92)$, $1e_u(1.87)$, $1e_u(1.87)$, $1b_{2g}(1.54)$, $1b_{2u}(0.46)$, $1e_g(0.13)$, $1e_g(0.13)$, $1a_{2u}(0.08)$, $2b_{1u}(0.02)$, $2b_{1g}(0.02)$.

tion number of 1.92. Next in strength is the pair of $\pi-$orbitals, $1e_u$, with a total occupation number of 3.74. Finally, the $\delta-$bonding orbital is occupied with 1.54 electrons. The corresponding antibonding orbitals have occupation numbers two minus that of the bonding orbital.

So, is this a quadruple bond? Formally it would seem so, because we have four bonding orbitals. But we remember from the preceding discussion that a bond is broken if the bonding and antibonding orbitals have the same occupation number one and it is fully formed when the bonding orbital is occupied by two electrons. Here we clearly see intermediate situations. The bond formation varies in the order: $\sigma > \pi > \delta$. Thus it does not seem reasonable to talk about a quadruple bond. If we define the covalent bond order for the orbital pairs i, BO_i, according to equation (23), we obtain: $BO_\sigma = 0.92$, $BO_\pi = 1.75$, and $BO_\delta = 0.54$. The summed bond order is 3.21, which is considerably less than four. It seems more appropriate to say that $[Re_2Cl_8]^{2-}$ has an effective triple bond. The weak $\delta-$bond is reflected in the electronic spectrum of the ion, which shows a transition at 14700 cm^{-1} due to the excitation $\delta \rightarrow \delta^*$ [35]. It is clear that the weak multiple bonding, occurring between transition metals in bimetallic systems, can only be understood in a multiconfigurational framework that allows the natural orbitals to have occupation numbers different from two and zero. This is a general finding for such complexes. It was earlier demonstrated for the diatomic Cr_2. More details about the Re complex will be published separately [33].

8 BLUE COPPER PROTEIN MODELS

The earlier sections of this chapter have been mostly concerned with the multiconfigurational description of the electronic structure of compounds involving a transition metal. In this final section, we goal is slightly different. We shall show an example, where the approach has been used to explain the bonding and spectroscopic properties in an important class of transition metal compounds, the so called blue copper proteins. The emphasis will now be on the results obtained and the comparison of different quantum chemical methods. Only a brief summary can be given here and the reader is referred to the original literature for more details.

Blue copper proteins transfer electrons between various biological systems, e.g. between the two photosystems in photosynthesis (plastocyanin). They are characterized by a number of unusual properties, viz. a bright blue color, an unusually high reduction potential, and distinctive electronic spin resonance spectra. The active site of these proteins consists of a copper ion bound to the protein in a trigonal geometry involving one cysteine and two histidine residues. The coordination sphere is normally completed by one or two weak axial ligands, e.g. methionine, glutamine, or a back-bone carbonyl group. The reason for the unusual properties and the strange geometry has been much discussed, but it seems now generally accepted that it comes mostly from the choice of metal ligands (in particular the cysteine thiolate ligand), rather than from mechanical strain enforced by the protein [36, 37, 38].

symmetry).

8.1 CuSH

Let us first look at the very simple $CuSH^{0/+}$ model as a representative of the important Cu^{2+} + S^{-} interaction of the blue copper proteins. This system is so small that it can be studied with most theoretical methods and with extended basis sets. We have studied three states of this model (neutral CuSH and $CuSH^{+}$ in the $^2A'$ and $^2A''$ states) [39]. All three states give similar results and a typical example is given in Table 1. From this comparison, it can be seen that the HF and CASSCF methods give poor geometries and energies. On the other hand, the MP2, CCSD(T) and CASPT2 methods give similar results, which indicates that the system is not especially multiconfigurational in nature. This is confirmed by the weight of the major CF, which is 0.96. The three DFT functionals tested give quite differing results, especially for the Cu–S bond length. B3LYP, seems in general to give the best results, although the Cu–S bond length is often somewhat too long with this method. A notable result for this model is the strong basis-set dependence of the CASPT2 method. Whereas the DFT results change very little (less than 1 pm and 1° when the basis set is enlarged, the CASPT2 geometry change by up to 8 pm and 4° when the basis set is enlarged from ANO–S to ANO–L [39]. This is a typical feature of wave function based methods, where the correlation energy is computed in a CI framework. The DFT method, which is based on the density alone, depneds much less on the basis set.

Table 1: The structure of the $^2A''$ state of $CuSH^+$, optimised with various methods and an ANO–S basis set (Cu: $17s12p9d4f/6s4p3d2f$, C: $13s10p4d/4s3p2d$, H: $7s3p/2s1p$). Distances in pm, angle in degrees, energy difference to the $^2A'$ state in kJ/mole.

Method	Cu–S	S–H	Cu–S–H	ΔE
HF	243.1	133.5	100.1	66
CASSCF	236.7	134.0	100.6	67
LDA	207.8	137.3	95.1	94
BP86	213.3	136.8	95.8	91
B3LYP	217.7	135.5	97.0	86
MP2	218.7	135.7	98.2	92
CCSD(T)	219.2	136.2	96.9	93
CASPT2	219.5	135.7	97.5	81
CASPT2/ANO–L[a]	214.8	134.6	97.9	86

[a] Cu: $21s15p10d6f4g/7s6p5d4f3g$, C: $17s12p5d4f/6s5p4d3f$, H: $8s4p3d/3s2p1d$

8.2 $Cu^{2+}(NH_3)_3X$

Next, we will look on complexes of the form $Cu^{2+}(NH_3)_3X$, where X is related to the thiolate ligand in the blue copper proteins, e.g. SH^-, OH^-, SeH^-, PH_2^- and Cl^-. Such complexes have been employed to explain why the blue copper proteins exhibit a trigonal structure, whereas most Cu(II) complexes assume a tetragonal structure [40]. For all these complexes, local minima representing both a tetragonal and a trigonal structure could be optimized. However, the relative stability of the trigonal structure increases as we move down and to the left in the periodic table, as can be seen in Table 2. It is also stabilized by negatively charged X ligands. The relative energies were calculated with both the CASPT2 and B3LYP methods. The two methods give rather similar results, with maximum and average differences of 18 and 8 kJ/mole, and they therefore give the same predictions of the most stable structure for all complexes, except for the two complexes where the two geometries are almost degenerate, $Cu(NH_3)_3(SH)^+$ and $Cu(NH_3)_3(PH_2)^+$.

Relativistic corrections (Darwin contact and mass–velocity terms calculated at the CASSCF level) are also given in the table. For most complexes, this correction is small and insignificant. However, for three complexes ($Cu(NH_3)_3(SH)^+$, $Cu(NH_3)_3(SeH)^+$, and $Cu(NH_3)_2(SH)(SH_2)^+$), the corrections are large (14–16 kJ/mole) and positive (favoring the tetragonal state). The reason for this is that relativistic corrections in general favor the structure with the lowest Cu $3d$ population. For the three complexes exhibiting large relativistic effects, the Cu $3d$ population for the tetragonal structure is 9.3–9.4, whereas it is 9.9 for the trigonal structure. For all the other com-

Table 2: Energy difference (kJ/mole) between the trigonal and tetragonal structures of the various model complexes.

Model	B3LYP	CASPT2	CASPT2 + Rel. Corr.
$Cu(NH_3)_4^{2+}$	46.0	42.8	42.2
$Cu(NH_3)_3(OH_2)^{2+}$	33.9	33.9	33.5
$Cu(NH_3)_3Cl^+$	38.2	49.3	47.4
$Cu(NH_3)_3(OH)^+$	19.7	37.6	35.9
$Cu(NH_3)_3(SH)^+$	3.1	-1.7	14.4
$Cu(NH_3)_3(SeH)^+$	-5.8	-18.2	-4.7
$Cu(NH_3)_3(PH_2)^+$	2.6	-4.4	-5.1
$Cu(NH_3)_2(SH)(SH_2)^+$	-12.6	-21.1	-7.0

plexes the CASSCF Cu $3d$ are similar for the tetragonal and the trigonal structures, either close to 9.3 or close to 9.9 (representing either d^9 or d^{10} states. This is not in accordance with the B3LYP results, where the Cu $3d$ populations are always similar (within ~ 0.1) for the two geometries, but it varies continuously between 9.3 and 9.7 (in general, it is lower for complexes with stable tetragonal states and higher for those with more stable trigonal states). This gives also an explanation to the tetrahedral distortion of the complexes with stable trigonal structures (both trigonal and tetrahedral): In the latter complexes much charge is donated from the large, soft, and polarizable negatively charged X ligand, giving rise to an electronic structure close to Cu^+, which is closed-shell (d^{10}) and therefore prefers a tetrahedral structure.

8.3 Electronic Spectra

Finally, we will discuss the electronic spectra of blue copper proteins. The absorption spectrum of plastocyanin, the best studied blue copper protein, is dominated by a bright band at 16 700 cm^{-1} (600 nm), giving rise to its bright blue color. However, a more thorough investigation of the experimental spectrum identifies at least six more absorption bands below 22 000 cm^{-1}, as is shown in Table 3 [41]. Several different methods have been used to interpret this spectrum, ranging from the semi-empirical CNDO/S method, over various DFT methods (Xα and time-dependent B3LYP calculations) to CASPT2 [42, 43, 41, 44, 45]. The results of the various calculations are also shown in Table 3 together with calculated oscillator strengths and an assignment of the various excitations.

All methods agree that in the ground state, the singly-occupied orbital is comprised of the Cu $3d_{xy}$ orbital and a S_{Cys} $3p$ orbital, forming an antibonding π interaction. The bright blue line arises from the excitation to the corresponding π *bonding* interaction, and its large intensity arises from the strong overlap between these two orbitals. This interaction also explains the trigonal structure of the plastocyanin site: By the π bond, S_{Cys} overlaps with two of the four lobes of the Cu $3d_{xy}$ orbital. The two histidine ligands form normal σ bonds to copper, overlapping with the remaining two lobes of the singly-occupied Cu $3d_{xy}$ orbital, whereas any additional ligand (methionine in plastocyanin) can only overlap with doubly occupied orbitals, and therefore forms weak axial interactions at long distances.

The normal Cu–S_{Cys} σ antibonding interaction is found as the first excited state in plastocyanin, at an excitation energy of 5 000 cm^{-1}. In some other proteins, e.g. nitrite reductase, this state becomes the ground state, giving rise to a strongly tetrahedrally distorted (owing to the charge transfer from S_{Cys}) tetragonal structure with σ bonds to all four ligands [45]. This state overlaps strongly with the corresponding σ bonding interaction, found at slightly higher energy than the π bond (21 900 cm^{-1} in nitrite reductase), giving this enzyme a green colour [46]. Other proteins exist that have intermediate structures and spectra, e.g. cucumber basic protein and pseudoazurin [45]. Moreover, various mutant proteins have been constructed with other ligand sets (but still a cysteine ligand) that have more tetragonal structures and even brighter excitations to the Cu–S_{Cys} σ orbital, giving them a yellow colour. In fact, the intensity ratio between the yellow and blue bands of all blue copper proteins can be rationalized by the transition of the structure from trigonal to tetragonal, e.g. as described by the angle between the planes defined by the N–Cu–N and S_{Cys}–Cu–S_{Met} atoms [45].

Table 3 shows that the accuracy of the CASPT2 method is impressive for this complicated system (a chromophore in a protein); The six lowest excitations are calculated with an error less than 1000 cm^{-1}. Owing to the size of the system, several approximations had to invoked to make the calculations possible. The chromophore was modelled by $Cu(imidazole)_2(SH)(SH_2)^+$, at the crystal geometry and with a point-charge model of the surrounding protein. However, this model is too small to give accurate results. Therefore, the excitation energies have been corrected (by up to 2600 cm^{-1}) for truncation effects by using data from the $Cu(imidazole)_2(SCH_3)(S(CH_3)_2)^+$, optimised

Table 3: The experimental spectrum of plastocyanin [41] compared to spectra calculated with the Xα, CASPT2, and time-dependent B3LYP methods [41, 44, 47]. All excitation energies are given in cm^{-1}. Significant oscillator strengths are indicated in parenthesis. The assignment is based on the CASPT2 calculations (invoking a coordinate system where the Cu ion is at the origin, the z-axis is along the Cu–S_{Met} bond, and the Cu–S_{Cys} bond is situated in the xy-plane). Two excitations studied with the CASPT2 method could only be studied by severe approximations (see the text) and are therefore marked by square brackets.

Experimental	CASPT2	B3LYP	Xα	Assignment
5 000	4 119	4 206	4 527	σ^*
10 800 (.0031)	10 974	9 441 (.0013)	8 691	d_{z^2}
12 800 (.0114)	13 117 (.0015)	12 827 (.0142)	11 942 (.046)	d_{yz}
13 950 (.0043)	13 493 (.0003)	13 673 (.0010)	15 064	d_{xz}
16 700 (.0496)	17 571 (.1032)	18 364 (.0733)	16 940 (.078)	π
18 700 (.0048)				
21 390 (.0035)	20 599 (.0014)	20 267 (.0002)	25 313	σ
23 440	[31 264]	20 806 (.0003)	15 895,36 700	Met
32 500	[34 992]	21 327 (.0006)	14 770,52 894	His

with the B3LYP method and C_s symmetry. Moreover, the calculations had to be performed with quite small basis sets, e.g. without polarising functions on the N, C and H atoms.

The two excitations with the highest energy (charge-transfer excitations to the methionine and histidine residues, respectively) could only be studied with the symmetric $Cu(imidazole)_2(SCH_3)(S(CH_3)_2)^+$ model at the optimised geometry. Therefore, these excitation energies are much less accurate, especially for the former excitation, which is very sensitive to the geometry of the model and also to the size of the basis sets. Finally, it should be noted that our assignment left one band unassigned, mainly on the basis that this band is not present in the spectrum of the related protein nitrate reductase [46, 45].

The plastocyanin spectrum calculated with the time-dependent B3LYP method (using the $Cu(imidazole)_2(SCH_3)(S(CH_3)_2)^+$ model optimised with B3LYP without symmetry; no point-charge model) is also included in Table 3 [47]. It can be seen that the result is quite similar to both the CASPT2 and the experimental results for the six lowest excitatons; the largest difference to the CASPT2 is 1 500 cm^{-1} for the second excitation and the largest difference to experiments is 1 700 cm^{-1} for the bright blue line. However, for the true charge-transfer excitations to the methionine and histidine ligands, the difference is much larger. The B3LYP calculations show one excitation to methionine at 21 327 cm^{-1}, compared to the experimental line at 23 440 cm^{-1}, and the CASPT2 result at 31 264 cm^{-1}. However, as was discussed above, for this excitation the CASPT2 results are not reliable. Similarly,

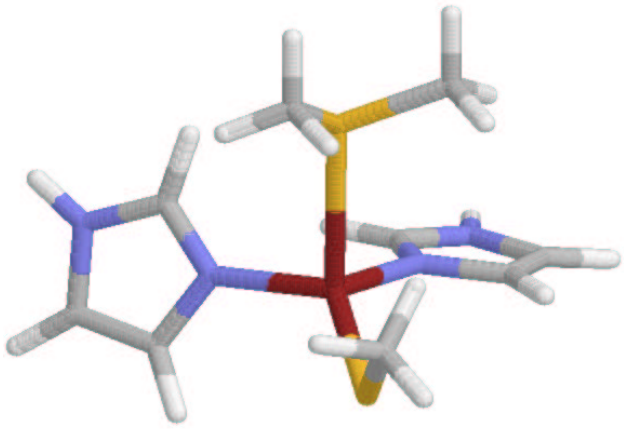

Figure 8: One of the models used in the study of the active site in the blue copper protein plastocyanin. Histidine ligands have been replaced with imidazole, cysteine with SCH_3^- and methionine with $S(CH_3)_2$.

B3LYP gives four excitations to the two histidine residues, two around 21 500 cm^{-1}, and two close to 35 500 cm^{-1}, all with a low calculated intensity. In the experimental spectrum, there is only one line at 32 500 cm^{-1}, and with CASPT2, only one excitation could be studied, giving an energy of 34 992 cm^{-1}. Thus, these results indicates that B3LYP gives rise to spurious charge-transfer excitations. Similar results have been obtained also for other (mostly organic) models (see for example the discussion of charge transfer bands in poly-peptides in Ref.[48]).

Finally, Table 3 also contains excitations for plastocyanin calculated with the density functional Xα method [41]. Once again, the result is similar to the other calculations and experiments for the six lowest excitations, whereas the discrepancy is much larger for the charge-transfer exciations. In general, Xα seems to give the least accurate results, except for the blue line (which may be because the method was parameterised to give the correct covalency of Cu–S_{Cys} bond). It should also be noted that the authors of this investigation made a different assignment of several bands in the spectrum [41].

In conclusion, we have seen that it is possible to study the spectrum of a chromophore in a protein with theoretical methods. CASPT2 seems to give the most accurate results, provided that a reasonable chemical model can be studied and proper active orbitals can be selected (five Cu $3d$ orbitals, five correlating Cu $3d'$ orbitals, and all orbitals involved in charge-transfer excitations). DFT, especially the time-dependent methods also gives reasonable results at a much lower cost and with a smaller basis-set dependence. It should be noted, however, that the assignment of the various excitations are

much easier to perform at the CASPT2 level than with DFT (the orbitals are more pure).

9 CONCLUSIONS

In this chapter we have tried to illustrate through some examples how a multiconfigurational model describes the electronic structure in coordination compounds. The key concept has been the NOs, which are the generalization of the HF orbitals to a situation where more than one electronic configuration is needed to describe the electronic structure. The examples (with the exception of the blue proteins) have been confined to the ground state. It is, however, evident that the multiconfigurational is even more essential in discussions of excited states and photochemistry.

Many theoretical studies of coordination compounds are today successfully performed using DFT. This is all good as long as one is aware of the pitfalls within this approach. The problem of charge-transfer processes was mentioned above. The definition of spin and the inclusion of spin-orbit coupling in heavier systems is another problem, which is of major concern in studies of electronic spectroscopy and photochemical reactions. Strongly degenerate situations can hardly be treated with DFT. One example is the Cr_2 molecule, which was discussed above. We have also tried to use DFT for the $[Re_2Cl_8]^{2-}$ ion, but failed to converge the calculations.

The virtue of a wave function based multiconfigurational approach is the

complete generality, meaning that any type of electronic structure may be studied with exactly defined spin and other symmetry properties. The major problem with the approach is the size of the active space, which limits the possibilities to compute the effects of dynamic electron correlation. Today the only possible approach for large molecules with many electrons is CASPT2, which is limited with respect to the active space and in some applications gives severe intruder state problems. It is hoped that in the near future we shall have access alternative methods where these limitations are removed.

References

[1] Hund, E. *Z. Physik*, **1927**, *40*, 742.

[2] Lennard-Jones, J. E. *Trans. Farady Soc.*, **1929**, *25*, 668.

[3] Mulliken, R. S. *Phys. Rev*, **1928**, *32*, 186.

[4] Heitler, W.; London, F. *Z. Physik*, **1927**, *44*, 455.

[5] Hartree, D. R. *The calculation of Atomic Strucutres.* Wiley Interscience, New York, 1957.

[6] Hückel, E. *Z. Physik*, **1930**, *60*, 423.

[7] Roothaan, C. C. J. *Revs. Mod. Phys.*, **1951**, *23*, 69.

[8] Löwdin, P.-O. *Phys. Rev.*, **1955**, *97*, 1474.

[9] Almlöf, J.; Ahlrichs, R. in *European Summer School in Quantum Chemistry, Book II*, Roos, B. O.; Widmark, P.-O., Eds. Lund University, Lund, Sweden, 2000.

[10] Roothaan, C. C. J. *Revs. Mod. Phys.*, **1960**, *32*, 179.

[11] Helgaker, T.; Jørgensen, P.; Olsen, J. *Molecular Electronic Structure Theory*. J. Wiley & Sons Ltd, Chichester, 2000.

[12] Lüthi, H. P.; Ammeter, J. H.; Almlöf, J.; Faegri, K. *J. Chem. Phys.*, **1982**, *77*, 2002.

[13] Andersson, K.; Roos, B. O. *Chem. Phys. Letters*, **1992**, *191*, 507.

[14] Froese-Fischer, C. *J. Phys. B*, **1977**, *10*, 1241.

[15] Roos, B. O.; Andersson, K.; Fülscher, M. P.; Malmqvist, P.-Å.; Serrano-Andrés, L.; Pierloot, K.; Merchán, M. in *Advances in Chemical Physics: New Methods in Computational Quantum Mechanics, Vol. XCIII:219–331*, Prigogine, I.; Rice, S. A., Eds. John Wiley & Sons, New York, 1996.

[16] Roos, B. O. in *Advances in Chemical Physics; Ab Initio Methods in Quantum Chemistry - II*, Lawley, K. P., Ed., chapter 69, p 399. John Wiley & Sons Ltd., Chichester, England, 1987.

[17] Roos, B. O. These calculations were performed with the CASSCF module of the MOLCAS quantum chemistry software. The active space chosen was the 3d and 4s orbital of each Cr atom (12) with 12 active electrons.

[18] Roos, B. O. in *European Summer School in Quantum Chemistry, Book II*, Roos, B. O.; Widmark, P.-O., Eds. Lund University, Lund, Sweden, 2000.

[19] Andersson, K.; Malmqvist, P.-Å.; Roos, B. O.; Sadlej, A. J.; Wolinski, K. *J. Phys. Chem.*, **1990**, *94*, 5483–5488.

[20] Andersson, K.; Malmqvist, P.-Å.; Roos, B. O. *J. Chem. Phys.*, **1992**, *96*, 1218–1226.

[21] Roos, B. O.; Andersson, K.; Fülscher, M. P.; Serrano-Andrés, L.; Pierloot, K.; Merchán, M.; Molina, V. *J. Mol. Struct. (Theochem)*, **1996**, *388*, 257–276.

[22] Chatt, J.; Duncanson, L. A. *J. Chem Soc.*, **1953**, p 2939.

[23] Dewar, M. J. S. *Bull. Soc. Chim. Fr.*, **1951**, p 79.

[24] Widmark, P.-O.; Roos, B. O.; Siegbahn, P. E. M. *J. Phys. Chem.*, **1985**, *89*, 2180.

[25] Widmark, P.-O.; Sexton, G. J.; Roos, B. O. *J. Mol. Struct. (Theochem)*, **1986**, *135*, 235.

[26] Pierloot, K.; Persson, B. J.; Roos, B. O. *J. Phys. Chem.*, **1995**, *99*, 3465–3472.

[27] Park, C.; Almlöf, J. *J. Chem. Phys.*, **1991**, *95*, 1829.

[28] Andersson, K.; Baryz, M.; Bernhardsson, A.; Blomberg, M. R. A.; Carissan, Y.; Cooper, D. L.; Cossi, M.; Fleig, T.; Flscher, M. P.; Gagliardi,

L.; de Graaf, C.; Hess, B. A.; Karlstrm, G.; Lindh, R.; Malmqvist, P.-.; Neogrdy, P.; Olsen, J.; Roos, B. O.; Schimmelpfennig, B.; Schtz, M.; Seijo, L.; Serrano-Andrs, L.; Siegbahn, P. E. M.; Stlring, J.; Thorsteinsson, T.; Veryazov, V.; Wierzbowska, M.; ; Widmark, P.-O. MOLCAS *Version 5.2*. Dept. of Theor. Chem., Chem. Center, Univ. of Lund, P.O.B. 124, S-221 00 Lund, Sweden, Lund, 2001.

[29] Pou-Amérigo, R.; Merchán, M.; Nebot-Gil, I.; Widmark, P.-O.; Roos, B. O. *Theor. Chim. Acta*, **1995**, *92*, 149.

[30] Widmark, P.-O.; Malmqvist, P.-Å.; Roos, B. O. *Theor. Chim. Acta*, **1990**, *77*, 291–306.

[31] Cotton, F. A.; Harris, C. B. *Inorg. Chem.*, **1965**, *4*, 330.

[32] Bertrand, J. A.; Cotton, F. A.; Dollase, W. A. *J. Am. Chem. Soc.*, **1963**, *85*, 1349.

[33] Gagliardi, L.; Roos, B. O. To be published.

[34] Cotton, F. A. *Inorg. Chem.*, **1965**, *4*, 334.

[35] Trogler, W. C.; Gray, H. B. *Acc. Chem. Res.*, **1978**, *11*, 232.

[36] Randall, D. W.; Gamelin, D. R.; LaCroix, L. B.; Solomon, E. I. *J. Biol. Inorg. Chem.*, **2000**, *5*, 16–29.

[37] Gray, H. B.; Malmström, B. G.; Williams, R. P. J. *J. Biol. Inorg. Chem.*, **2000**, *5*, 551–559.

[38] Ryde, U.; Olsson, M. H. M.; Roos, B. O.; Kerpel, J. O. A. D.; Pierloot, K. *J. Biol. Inorg. Chem.*, **2000**, *5*, 565–574.

[39] Ryde, U.; Olsson, M. H. M. *Int. J. Quantum Chem.*, **2001**, *81*, 335–347.

[40] Olsson, M. H. M.; Ryde, U.; Roos, B. O.; Pierloot, K. *J. Biol. Inorg. Chem.*, **1998**, *3*, 109–125.

[41] Gewirth, A. A.; Solomon, E. I. *J. Am. Chem. Soc.*, **1988**, *110*, 3811–3819.

[42] Larsson, S.; Broo, A.; Sjölin, L. *J. Phys. Chem.*, **1995**, *99*, 4860–4865.

[43] Penfield, K. W.; Gewirth, A. A.; Solomon, E. I. *J. Am. Chem. Soc.*, **1985**, *107*, 4519–4519.

[44] Pierloot, K.; De Kerpel, J. O. A.; Ryde, U.; Roos, B. O. *J. Am. Chem. Soc.*, **1997**, *119*, 218–226.

[45] Pierloot, K.; De Kerpel, J. O. A.; Ryde, U.; Olsson, M. H. M.; Roos, B. O. *J. Am. Chem. Soc.*, **1998**, *120*, 13156–13166.

[46] LaCroix, L. B.; Shadle, S. E.; Wang, Y.; Averill, B. A.; Hedman, B.; Hodgson, K. O.; Solomon, E. I. *J. Am. Chem. Soc.*, **1996**, *118*, 7755–7768.

[47] Borin, A. C.; Olsson, M. H. M.; Ryde, U.; Roos, B. O.; Pierloot, K. The geometry and electronic spectrum of Cu-substituted alcohol dehydrogenase. To be published, 2002.

[48] Tozer, D. J.; Amos, R. D.; Handy, N. C.; Roos, B. O.; Serrano-Andrés, L. *Mol. Phys.*, **1999**, *97*, 859–868.

10 Figure Captions

Fig. 1: Natural orbital occupation numbers for the active orbitals in C_4H_8 as a function of the distance between the two C_2H_4 fragments. The NOs are shown in Fig. 2. The occupation number profiles of the four orbitals (1-4) have the following colors: black, red, magenta, and blue.

Fig. 2: The four natural orbitals in C_4H_8, which change character during the reaction. The distance between the two ethene fragments is 2 Å.

Fig. 3: Natural orbital occupation numbers for the bonding and antibonding orbitals in Cr_2 as a function of the distance between the two atoms.

Fig. 4: The partitioning of the orbital space into inactive, active and virtual in the CASSCF method.

Fig. 5: Natural orbitals in the NiC_2H_4 molecule. Counted from left to right and from bottom up, the orbitals are (occupation numbers within parenthesis): $9a_1$ (2.00), $10a_1$ (1.98), $11a_1$ (1.97), $12a_1$ (0.03), $13a_1$ (0.02), $5b_2$ (1.91), $6b_2$ (0.09), $4b_1$ (1.98), $5b_1$ (0.02), $2a_2$ (1.98), $3a_2$ (0.02).

Fig. 6: Natural orbitals in the Ferrocene molecule. Counted from right to left and from top down, the orbitals are (occupation numbers within parenthesis): $8a_1'(1.96)$, $4e_1''(1.95)$, $4e_1''(1.95)$, $4e_2'(1.94)$, $4e_2'(1.94)$, $5e_1''(0.07)$, $5e_2'(0.05)$, $5e_2'(0.05)$, $9a_1'(0.03)$, $5e_1''(0.07)$.

Fig. 7: Natural orbitals in the $[Re_2Cl_8]^{2-}$ ion. Counted from right to left and from top down, the orbitals are (occupation numbers within parenthesis):

$1b_{1u}(1.98)$, $1b_{1g}(1.98)$, $1a_{1g}(1.92)$, $1e_u(1.87)$, $1e_u(1.87)$, $1b_{2g}(1.54)$, $1b_{2u}(0.46)$, $1e_g(0.13)$, $1e_g(0.13)$, $1a_{2u}(0.08)$, $2b_{1u}(0.02)$, $2b_{1g}(0.02)$.

Fig. 8: One of the models used in the study of the active site in the blue copper protein plastocyanin. Histidine ligands have been replaced with imidazole, cysteine with SCH_3^- and methionine with $S(CH_3)_2$.

March 26, 2002

Björn O. Roos and Ulf Ryde
Department of Theoretical Chemistry, Chemical Center,
P.O.Box 124, S-221 00 LUND, Sweden
e-mail: Bjorn.Roos@teokem.lu.se; Ulf.Ryde@teokem.lu.se
Phone: +46-46-222 8251; Fax: +46-46-222 4543